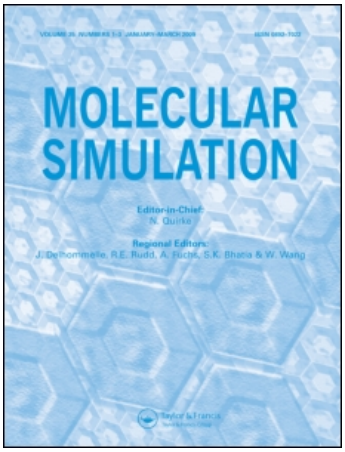

Molecular Simulation
Publication details, including instructions for authors and subscription information:
http://www.informaworld.com/smpp/title~content=t713644482

Micro-phase separation and configuration of ABC triblock copolymer in ultra-thin film by Monte Carlo simulation

X. Xiao[a]; Y. Huang[a]; H. Liu[a]; Y. Hu[a]
[a] Department of Chemistry, State Key Laboratory of Chemical Engineering, East China University of Science and Technology, Shanghai, China

To cite this Article Xiao, X. , Huang, Y. , Liu, H. and Hu, Y.(2007) 'Micro-phase separation and configuration of ABC triblock copolymer in ultra-thin film by Monte Carlo simulation', Molecular Simulation, 33: 13, 1083 — 1091
To link to this Article: DOI: 10.1080/08927020701579329
URL: http://dx.doi.org/10.1080/08927020701579329

Molecular Simulation, Vol. 33, No. 13, November 2007, 1083–1091

Taylor & Francis
Taylor & Francis Group

Micro-phase separation and configuration of ABC triblock copolymer in ultra-thin film by Monte Carlo simulation

X. XIAO, Y. HUANG*, H. LIU* and Y. HU

Department of Chemistry, State Key Laboratory of Chemical Engineering, East China University of Science and Technology, Shanghai 200237, China

(Received March 2007; in final form July 2007)

A Monte Carlo simulation using the bond fluctuation and cavity diffusion algorithms was adopted to investigate the micro-phase separation of ABC triblock copolymer in ultra-thin film on simple cubic lattice. Simulations reveal that the morphologies of ABC copolymer films are dependent on not only the volume fraction of the middle block B (f_B) but also on the ratio of interaction between different kinds of blocks ($\varepsilon_{(AC)}/\varepsilon_{(AB)}$). As for the molecular orientation, the copolymers stretch parallel to the flat surface at lower f_B, but tend to align perpendicularly along z direction at higher f_B. Furthermore, the chain configuration was discussed in detail. Smaller $\varepsilon_{(AC)}/\varepsilon_{(AB)}$ is beneficial to the formation of a "loop" configuration, whereas, larger $\varepsilon_{(AC)}/\varepsilon_{(AB)}$ would result in a "bridge" configuration of ABC triblock copolymer chains. The formation of micro-phase structures was illustrated intuitively by the molecular orientation and the chain configuration.

Keywords: ABC triblock copolymer; Ultra-thin film; MC simulation; Micro-phase separation; Configuration

1. Introduction

Block copolymers have been applied widely as templates for their amazing ability to be self-assembled into a variety of ordered microstructures [1,2] in the preparation of nano-materials such as organic photoelectrical nano-materials [3], biological medicine materials [4] and photonic crystals [5], etc. The various microstructures can be effectively controlled by various factors such as the composition of copolymer [6], temperature [7], nature of the blocks, annealing, quenching [8] and so on. Due to the extensive applications of block copolymer film, it is meaningful to study the micro phase separation of block copolymer film in detail [9–12].

Various ordered microstructures such as lamellar, cylindrical, spherical, diamond, gyroid and double-diamond have been found in ABC triblock copolymer melt via self-aggregation [13,14]. To study the disordered phase and the weak segregation phenomenon of the ordered phases, several mathematical methods including Γ—convergence theory, energy comparison method and rigorous singular perturbation analysis were adopted in self-consistent field theory (SCFT) by Ren and Wei [15]. Feng *et al.* [16] and Huang *et al.* [17] simulated the morphologies of ABA and ABC triblock copolymer melt films confined between two impenetrable walls via MC simulation on a cubic lattice, some microphases such as parallel, perforated, mesh-like and normal lamellae were found at varying film thickness. Huang *et al.* [17] also studied the "bridge" configuration of triblock copolymer chains in detail. More theoretical and simulation studies on the micro-phase separation of block copolymer can be found in references [18–20].

In this work, particular emphasis is placed on identifying the formation for the various micro-phase morphologies of ABC triblock copolymer in ultra-thin film in detail via Monte Carlo simulation. Here the so-called ultra-thin film is referred to the less film thickness (L_z) than L_0 (L_0: lamellar repeat spacing) [21]. Following this method, we simulate the box with a size of $44 \times 44 \times 44$ with the periodic boundary conditions along all the directions, and after several runs generating from the different initial states, L_0 in the bulk phase can be calculated approximately in the range of 10–14 for all the different $A_nB_mC_n$ $(N = 2n + m = 21)$ that will be examined later. As a consequence, our simulated system with L_0 and $L_z = 10$ is just involved into the ultra-thin film. Based on the molecular orientation and the chain configuration, the micro-phase separation of ABC ultra-thin film is explained. The outline of this paper is arranged

*Corresponding authors. Tel/Fax: + 86-21-64252921. Email: hlliu@ecust.edu.cn, huangym@ecust.edu.cn

Molecular Simulation
ISSN 0892-7022 print/ISSN 1029-0435 online © 2007 Taylor & Francis
http://www.tandf.co.uk/journals
DOI: 10.1080/08927020701579329

as follows. In section 2, a brief description about the simulation model and method is introduced. In addition, simulation parameters are introduced to characterize the behavior of ABC triblock copolymer. In section 3, the micro-phase morphologies and molecular orientation of ABC ultra-thin films at varying f_B are discussed. Subsequently in section 4, we examined the micro-phase structures and the chain configuration of ABC triblock copolymer films at varying $\varepsilon_{(AC)}/\varepsilon_{(AB)}$. Finally, the conclusions are given in section 5.

2. Physical model and parameters

The bond fluctuation model [22–24] and cavity diffusion algorithm [25] were adopted in this work. A cubic lattice model with a size of $L_x \times L_y \times L_z = 66 \times 66 \times 10$ lattice parameter was used in simulation, where L_x, L_y and L_z are the box dimensions in x, y and z directions, respectively. Periodic boundary conditions were adopted in the x and y directions, while in the z direction, two hard neutral walls were located at $z = 0$ and $z = L_z + 1$. Every segment of A, B and C is spherical with diameter 1 × lattice parameter. Every lattice point was occupied either by a segment (A, B or C) or by a vacancy. In the simulations, only the nearest neighbor interaction was taken into account, and the vacancy was neutral without any interaction with both segments and walls. The length of symmetric $A_nB_mC_n$ triblock copolymer chain was $N = 2n + m = 21$ and the density in box was set up to 0.9545. In simulations, the micro-phase morphologies of ABC ultra-thin films were repeated several runs using the same molecular parameters but starting from different initiations. In order to test whether the system has reached equilibrium or not, the simulated result was recorded and imaged every 1,000,000 Monte Carlo Steps (MCSs). It is found that after running about 24,000,000 MCSs, the system reached the equilibrium state identified by comparing all the recorded images. If the images were going to reach the stable structure, the equilibrium state was estimated.

As for the evolution of morphology of ABC ultra-thin film, it is convenient to explore from the molecular orientation and the chain configuration. The end-to-end distance, the mean square radius of the gyration [26,27], the molecular orientation and the chain configuration, were measured which are defined as follows:

End-to-end distance:

$$R=\left\langle \left\{ (1/M)\sum_{i=1}^{M}[(x_{iN}-x_{i1})^2+(y_{iN}-y_{i1})^2+(z_{iN}-z_{i1})^2] \right\}^{1/2} \right\rangle \tag{1}$$

where $\langle\cdot\rangle$ denotes the ensemble average, x_{i1}, y_{i1}, z_{i1} are the Cartesian coordinates of the first segment of ith polymer chain, x_{iN}, y_{iN}, z_{iN} are the spatial position of the Nth segment of ith polymer chain, namely the last segment; M is the number of polymer chains in the simulation box.

Mean square radius of the gyration:

$$R_g^2=\left\langle (1/M)\sum_{j=1}^{M}\left(\frac{1}{N}\sum_{i=1}^{N}[(x_{ji}-x_{jc})^2+(y_{ji}-y_{jc})^2+(z_{ji}-z_{jc})^2]\right)\right\rangle \tag{2}$$

where x_{ji}, y_{ji}, z_{ji} are the spatial position of the ith segment of jth polymer chain; and x_{jc}, y_{jc}, z_{jc} denote the Cartesian coordinates of the mass center of jth polymer chain.

Molecular orientation [28–30]

Since, the copolymer molecules highly anisotropic, a better examination of the state of them is to represent each molecule in terms of an equivalent moment of inertia of a spheroid [28]. In practice this means diagonalizing the moment of inertia tensor to obtain the principle moments I_{aa}, I_{bb} and I_{cc}, and three corresponding eigenvectors **a**, **b** and **c**, which lie along the principal axes of the spheroid. The moment of inertia tensor of molecule j is defined by

$$I_{j\alpha\beta} = \sum_i m_i\left(r_i^2\delta_{\alpha\beta} - r_{i\alpha}r_{i\beta}\right) \tag{3}$$

where α, $\beta = x$, y and z, $\delta_{\alpha\beta}$ is the Kronecker delta, $r_{i\alpha}$ is the distance in the α direction of segment i from the center of mass (c), m_i is the mass of ith segment of jth polymer chain and all the m_i are set equal to unity, and r_i^2 as a function of the distance to the center of mass (c) is employed. The sum is over all the segments of molecule j. The three corresponding eigenvalues are the respective principal moments of inertia I_{aa}, I_{bb} and I_{cc}, and the eigenvector **a** is the one that corresponds to the smallest eigenvalue I_{aa} and is referred to as the molecular long axes vector so as to establish the molecular orientation. The lengths of the semi-axis vectors are given by

$$a = \sqrt{5(I_{bb} + I_{cc} - I_{aa})/2N} \tag{4}$$

$$b = \sqrt{5(I_{aa} + I_{cc} - I_{bb})/2N} \tag{5}$$

$$c = \sqrt{5(I_{bb} + I_{aa} - I_{cc})/2N} \tag{6}$$

The lengths of the principal axes of the spheroid give estimates of the molecular "length", "width" and "breadth" which are respectively $2a$, $2b$ and $2c$.

In order to establish the orientations of the molecules with respect to the flat surface, it is convenient to define a correlation function to estimate the molecular orientation [28,31,32],

$$G_2(z) = \frac{3\langle \sin^2\theta(z)\rangle - 1}{2} \tag{7}$$

where z is the height position of the mass center c of the chains, and $\theta(z)$ is the orientation angle between

the molecular long axes vector **a** and the flat surface for the chains locating at a certain z. The value of $G_2(z)$ is limited to the $[-0.5,1.0]$ interval. If the molecular axes align parallel to the flat surface then $G_2(z) = -0.5$, if they orient perpendicularly to the flat surface then $G_2(z) = 1.0$, and if they are isotropic then $G_2(z) = 0$.

Chain configuration

In order to characterize the conformation of copolymer chains further, an interesting conformational quantity with respect to "loop" and "bridge" configurations of triblock copolymer was adopted by Huh and Jo [33] to explain the chain configuration intuitively. The angle ϕ between the vectors from the center of mass of block B to the centers of mass of respective A block and C block is used as the standard measure of chain configurations. Denoting the position vector of the centers of mass of these blocks as $\mathbf{r}_A$, $\mathbf{r}_B$ and $\mathbf{r}_C$, the equation is given as

$$\cos\phi = \frac{(\mathbf{r}_A - \mathbf{r}_B)\cdot(\mathbf{r}_C - \mathbf{r}_B)}{|\mathbf{r}_A - \mathbf{r}_B||\mathbf{r}_C - \mathbf{r}_B|} \tag{8}$$

Although, the segments site at the cubic lattice, it is also unconceivable that any two blocks might have their center of mass c at exactly the same site as a reason of the repulsion volume effect and the real number of $\mathbf{r}_A$, $\mathbf{r}_B$ and $\mathbf{r}_C$. When $\cos\phi \geq 0$, namely $0 \leq \phi < 90°$, the copolymer chain takes on a "loop" configuration as shown in figure 1(a); when $\cos\phi < 0$ as depicted in figure 1(b), namely $90° \leq \phi \leq 180°$, it takes on a "bridge" configuration. So it is easily understood that the copolymer chain of "loop" configuration is frizzier and the more sphericity than that of "bridge" configuration.

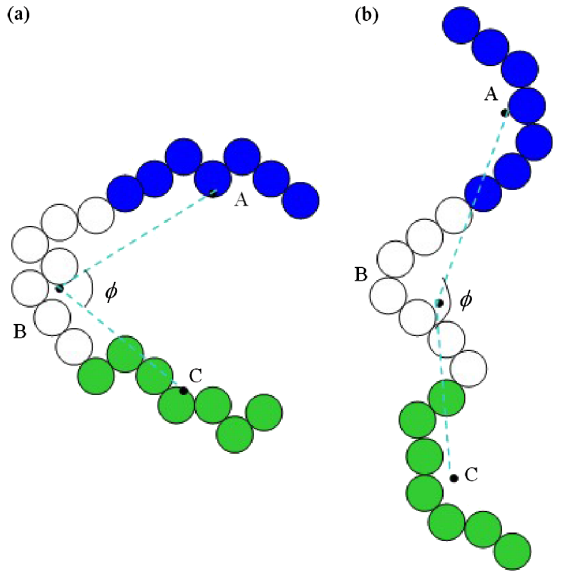

Figure 1. The chain configurations of $A_7B_7C_7$ triblock copolymer. (a) "loop"; (b) "bridge".

3. Molecular orientations in ultra-thin films vs. varying f_B

It is well known that the morphologies in confined micro-phase separated systems depend crucially on the relationship between the characteristic length of the corresponding bulk morphology and the film thickness [34]. Mismatch between the natural period of the bulk structure and film thickness causes either specific orientation of the structure with respect to the substrate or can even create new morphologies not existing in the bulk. In this work, the relationship between varying f_B and the micro-phase morphologies of copolymer ultra-thin film and the molecular orientations were investigated at $L_z/N = 0.4762$.

Figure 2 shows the micro-phase morphologies of symmetric $A_nB_mC_n$ film confined between two neutral walls with $\varepsilon_{AB} = \varepsilon_{BC} = \varepsilon_{AC} = 0.3$. When f_B is small, as shown in figure 2(a)–(c), the regular perpendicular lamellae impenetrate the whole ultra-thin film. The width of B micro-domain, which is uniformly located at the interfaces between A and C micro-domains, is notably increasing from the single string of pearls when $m = 1$ (figure 2(a)) to a narrow strip when $m = 5$ and 7 (figure 2(b),(c)). When f_B increases further, more disordered micro-phase morphologies are formed. When f_B is up to 0.6190 as shown in figure 2(e), the rich-B phase aggregates forming network. When $f_B = 0.8095$ or further, the rich-B phase expands through the whole film, the sizes of A and C domains shrinkage and tend to be dispersed in the rich-B matrix. Results of this work show good accordance with Bates and Fredrickson's [35] summary of the morphologies of ABC triblock copolymer, the lamella–sphere phase and the lamella–cylinder phase are obtained at low f_B. When f_B increases, the lamellar phase and the tri-continuous double-diamond phase are obtained under specific conditions.

Figure 3 exhibits the end-to-end distance $\langle R\rangle$ and the mean radius of gyration $\langle R_g^2\rangle$ with various f_B of the symmetric $A_nB_mC_n$ with the aim to reflect the stretch trend of the chains qualitatively. When f_B varies from 0.1 to 0.35, it is shown that the $\langle R\rangle$ curve appears a flat heave with a maximum at about $f_B = 0.2$. Correspondingly, the $\langle R_g^2\rangle$ curve also shows a higher peak in this interval. The larger $\langle R\rangle$ and $\langle R_g^2\rangle$ correspond to the more outspread of the copolymer chains. When f_B increases further, the $\langle R\rangle$ and $\langle R_g^2\rangle$ curves decline obviously indicating the decrease of the stretch capability of copolymer chains. It seems that the response of $\langle R\rangle$ to the change of f_B is not as sensitive as that of $\langle R_g^2\rangle$ in figure 3. As f_B is larger than 0.9, the sudden frustration of the two curves shows consistency with the micro-phase morphology shown in figure 2 (h), indicating that the copolymer chains could not bring on the micro-phase separation due to the extreme shortage of the two end-blocks. From the trend of $\langle R\rangle$ and $\langle R_g^2\rangle$ curves in figure 3, one can conclude that the less f_B is, the more outspread the copolymer chains are. This is because that the end blocks are more flexible than that of

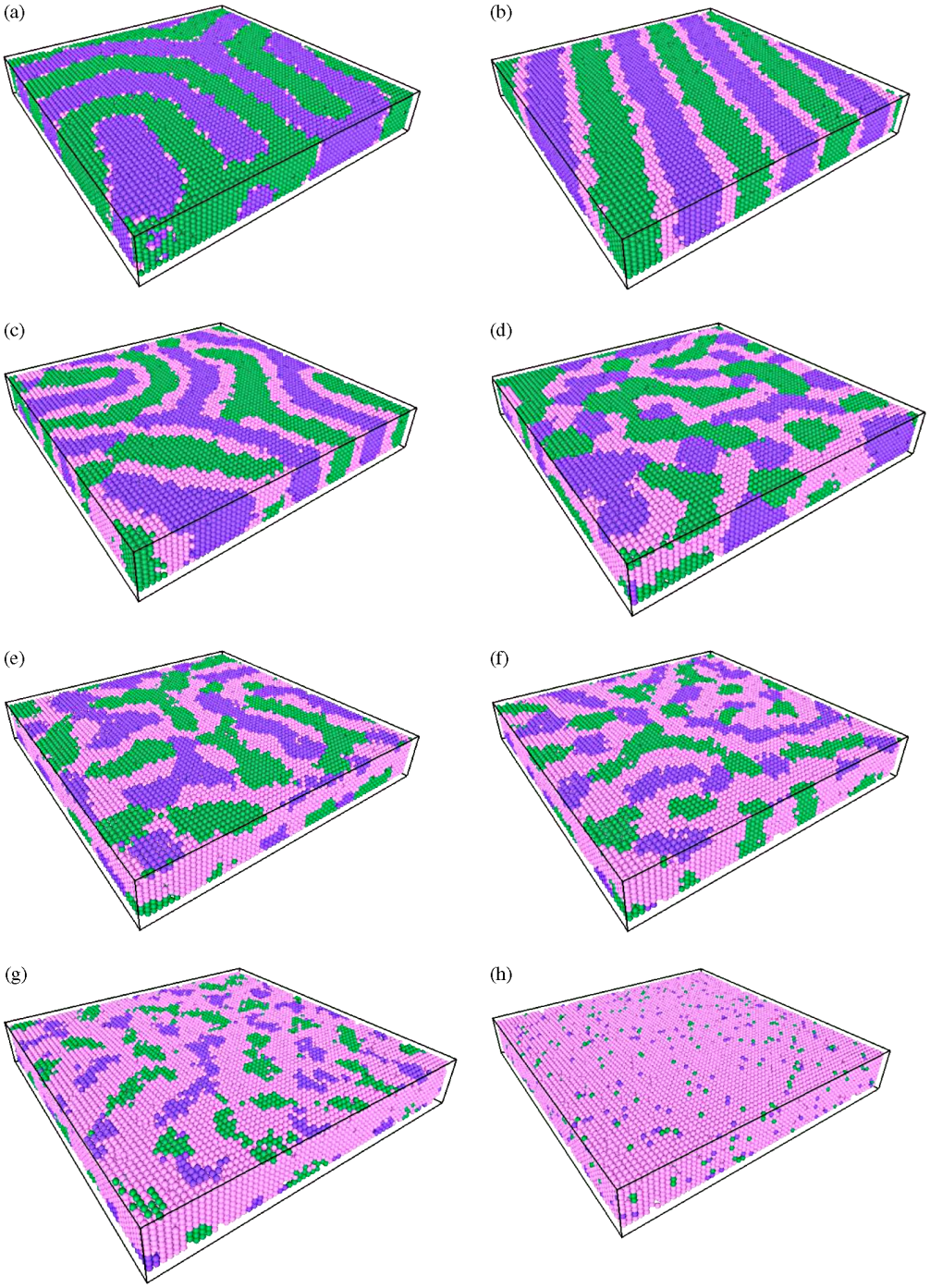

Figure 2. Micro-phase morphologies of symmetric $A_nB_mC_n$ film between two neuter walls, $\varepsilon_{AB} = \varepsilon_{BC} = \varepsilon_{AB} = 0.3$. Black: A blocks; White: B blocks; Gray: C blocks. (a) $m = 1, f_B = 0.0476$; (b) $m = 5, f_B = 0.2381$; (c) $m = 7, f_B = 0.3333$; (d) $m = 9, f_B = 0.4286$; (e) $m = 13, f_B = 0.6190$; (f) $m = 15, f_B = 0.7143$; (g) $m = 17, f_B = 0.8095$; (h) $m = 19, f_B = 0.9048$.

the middle blocks leading to the increase of the conformational and translational entropy of copolymer chains. The entropy dominates the micro-phase morphologies as well as the stretch of copolymer chains.

The aggregations and molecular orientations are reflected through the distribution of mass center c in the z direction as depicted in figure 4. $P\langle z(c)\rangle$ as a function of the statistical probability of mass center c at a distance z away from the bottom surface is imposed. From the figure 4, one can find that nearly uniform distribution of mass center c occurs among the middle layers of the copolymer film at the lower f_B, even though there are two low peaks nearby the two hard walls respectively (see $A_9B_3C_9$ and $A_7B_7C_7$). As f_B increases, the distribution of mass center c along the z direction tends to raise a notable peak in the middle layers of the ultra-thin film indicating that more and more mass centers of the chains converge towards the middle layers (see $A_5B_{11}C_5$ and $A_3B_{15}C_3$ and $A_2B_{17}C_2$). The height of the peak rises with the increasing f_B. It can be concluded that the mass centers c are

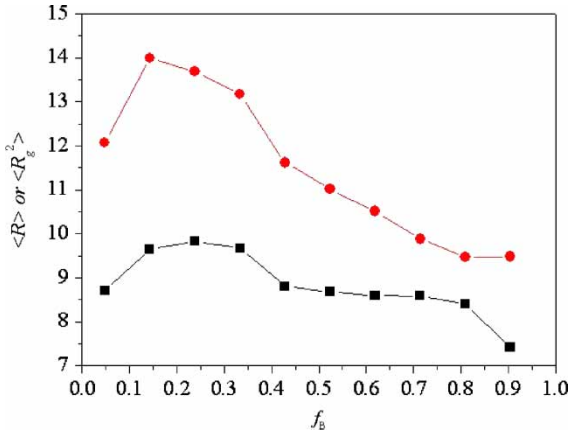

Figure 3. The relations between $\langle R\rangle$ and $\langle R_g^2\rangle$ with the various f_B ■: $\langle R\rangle$; ●: $\langle R_g^2\rangle$.

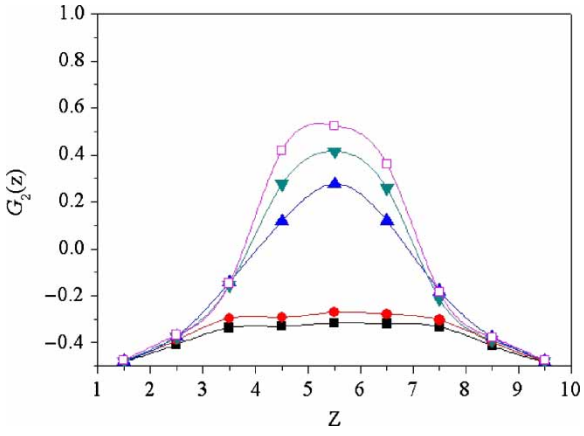

Figure 5. The statistical values of $G_2(z)$ along the z direction. ■: $A_9B_3C_9$; ●: $A_7B_7C_7$; ▲: $A_5B_{11}C_5$; ▼: $A_3B_{15}C_3$; □: $A_2B_{17}C_2$.

aggregated towards the middle layers as a result of the increase of f_B at a relative small L_z/N.

The correlation function $G_2(z)$ defined by equation (7) was used to study the molecular orientations per layer along the z direction directly, which is plotted in figure 5. For $A_2B_{17}C_2$ with large f_B, the $G_2(z)$ value of copolymer chains aggregating in the middle layers is up to more than 0.5, notably exceeding that of copolymer chains nearby the hard walls, -0.5. The nearer the walls, the lower the $G_2(z)$ value is. For $A_9B_3C_9$ with lower f_B, the lower $G_2(z)$ value appears through the whole ultra-thin film, in the middle region, $G_2(z)$ value falls rapidly close to -0.3. The results indicate that no matter what f_B is, most of the copolymer chains nearby the two hard walls align parallel to the flat surfaces characterizing by the lower $G_2(z)$ value. Whereas the $G_2(z)$ value of copolymer chains aggregating in the middle layers is much higher for the larger f_B indicating that almost all the copolymer chains in the middle layers tend to stretch by standing along the direction of z axis, relatively perpendicular to the flat surface. As for the smaller f_B, no matter where the copolymer chains are, the $G_2(z)$ value are all less than -0.3 through the whole film, thus all the copolymer chains orientate parallel to the flat surface. By comparing figure 5 with figure 4, it is shown that most of the copolymer chains are converged together towards the middle layers and stretched perpendicularly to the flat surface at large f_B (see $A_2B_{17}C_2$). Only a little of the copolymer chains nearby the two walls align parallel to the flat surfaces. In contrast, as f_B is small, for instance the $A_9B_3C_9$, nearly whole copolymer chains are stretched parallel to the flat surface and distributed uniformly in every layer of the ultra-thin film.

As f_B increases, the orientation transformation from parallel to relatively perpendicular is also the main factor resulting in the sharp decrease of $\langle R\rangle$ and $\langle R_g^2\rangle$. When the copolymer chains are relatively perpendicular to the flat surface, they are compelled forcedly by the two hard walls, therefore, they can not stretch naturally in the z direction. On the other hand, at lower f_B, the copolymer chains align parallel without suffering the repulsion from the hard walls which lead to the larger value of $\langle R\rangle$ and $\langle R_g^2\rangle$.

Figure 6 shows the $\langle P(\theta)\rangle$ distribution with varying f_B, where $\langle P(\theta)\rangle$ is the statistical probability of molecular orientation at θ. At low f_B, one can find a rapid decrease of

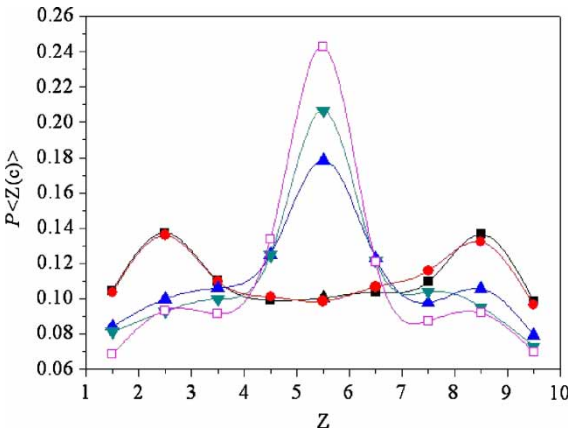

Figure 4. The distribution of mass center along the z direction. ■: $A_9B_3C_9$; ●: $A_7B_7C_7$; ▲: $A_5B_{11}C_5$; ▼: $A_3B_{15}C_3$; □: $A_2B_{17}C_2$.

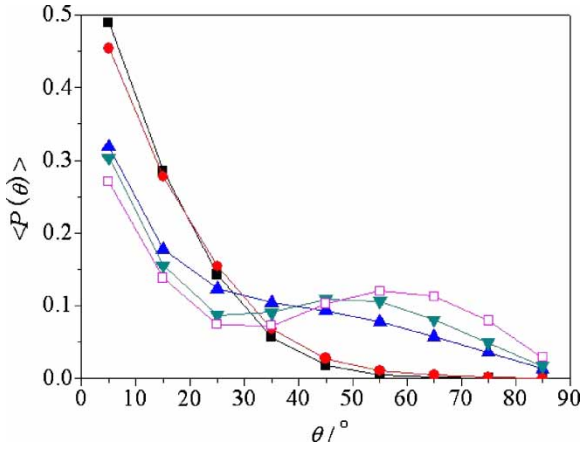

Figure 6. The distribution of $\langle P(\theta)\rangle$ with varying f_B. ■: $A_9B_3C_9$; ●: $A_7B_7C_7$; ▲: $A_5B_{11}C_5$; ▼: $A_3B_{15}C_3$; □: $A_2B_{17}C_2$.

$\langle P(\theta)\rangle$ with the increase of θ in the [10°,30°] interval, indicating that almost all the copolymer chains stretch at the low θ. On the contrary, there is great difference for large f_B systems. Although a drop of $\langle P(\theta)\rangle$ in the [10°,30°] interval is observed, the sum of $\langle P(\theta)\rangle$ after $\theta > 30°$ is still high close to 50%. Moreover, a jump of $\langle P(\theta)\rangle$ occurs at $\theta > 40°$, indicating the obvious increase in the amount of copolymer chains tilted at the relative high angle θ. Taking the $A_2B_{17}C_2$ as an example, a peak appears at the [50°,70°] interval. However, most of the copolymer chains are still orientated at low θ. Combined with Figures 4 and 5, it is concluded that nearly all the copolymer chains align parallel to the flat surface at low f_B, hence the orientation is concentrated at low angle. Whereas, at large f_B, only about 50% copolymer chains nearby the two hard walls still stretch parallel to the flat surface, the others aggregate in the middle layers orientated relatively perpendicular to the flat surface.

Figure 7 gives a qualitative sketch map of the molecular orientations and micro-phase morphologies in the ultra-thin films as a summary. When f_B is small, as shown in figure 7(a), the whole copolymer chains are stretched parallel to the flat surface and distributed uniformly in every layer, the perpendicular lamellae structures appears. When f_B is large, as shown in figure 7(b), the most mass centers of the chains are converged together towards the middle layers of the ultra-thin film, and are stretched relative perpendicularly to the flat surface. Only a little of copolymer chains nearby the two walls align parallel to the flat surface. For the relative perpendicular copolymer chains, they are compressed because of the repulsion from the hard walls. The perforated lamellae structure of rich-B phase in the middle layers is formed finally.

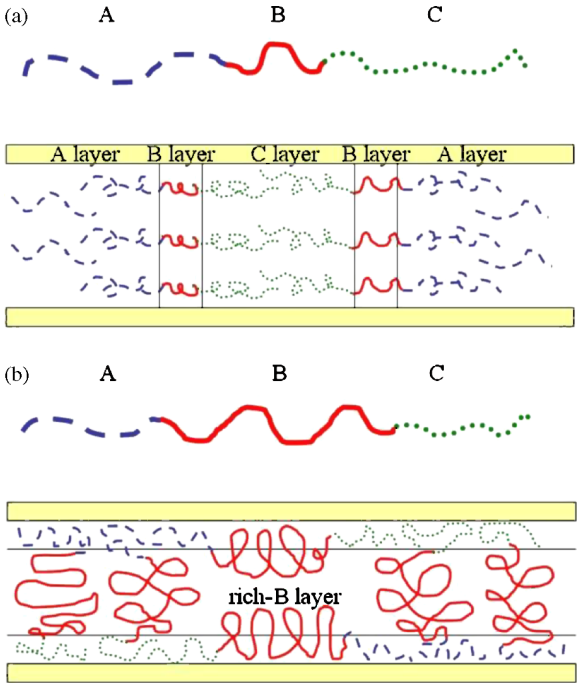

Figure 7. The sketch maps of the molecular orientations and micro-phase morphologies.

4. Chain configurations vs. varying $\varepsilon_{(AC)}/\varepsilon_{(AB)}$

To evaluate the effect of interactions between different kinds of blocks on the micro-phase morphologies, simulations were carried out for systems confined by neutral walls with $\varepsilon_{(BC)} = 0.3$ and a repulsive $\varepsilon_{(AB)}$. The influence of the ratio $\varepsilon_{(AC)}/\varepsilon_{(AB)}$ is shown in figure 8. When the end blocks A and C attract each other with negative $\varepsilon_{(AC)}$ and $\varepsilon_{(AC)}/\varepsilon_{(AB)}$, micro-phase separation between A and C is not formed, they are embedded mutually forming the continuous strip as shown in figure 8(a). Whereas the B phase domain is

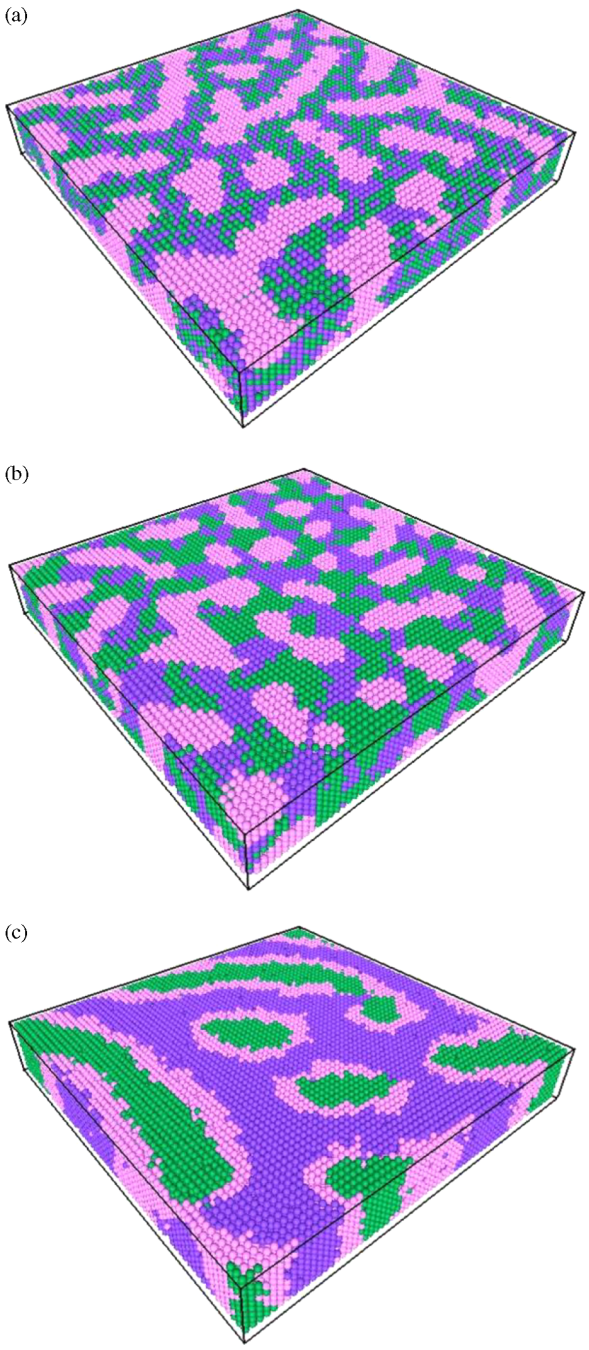

Figure 8. Micro-phase morphologies of $A_7B_7C_7$ with varying $\varepsilon_{(AC)}/\varepsilon_{(AB)}$. The walls are neutral, and $\varepsilon_{(BC)} = 0.3$. Black: A blocks; White: B blocks; Gray: C blocks. (a) $\varepsilon_{(AC)}/\varepsilon_{(AB)} = (-0.1)/0.3 = -0.333$; (b) $\varepsilon_{(AC)}/\varepsilon_{(AB)} = 0.1/0.5 = 0.2$; (c) $\varepsilon_{(AC)}/\varepsilon_{(AB)} = 0.5/0.3 = 1.6667$.

irregularly dispersed and surrounded by those continuous strips. When A and C is slightly repulsive with $\varepsilon_{(AC)} = 0.1$ and $\varepsilon_{(AC)}/\varepsilon_{(AB)} = 0.2$, as shown in figure 8(b), the end blocks are separated into small aggregations, the three blocks are dispersed irregularly forming the morphology that looks like "tricolor checkerboard". When the repulsive interaction between A and C is further enhanced, $\varepsilon_{(AC)}$ jumps to 0.5, $\varepsilon_{(AC)}/\varepsilon_{(AB)} = 1.6667$, as shown in figure 8(c), local perpendicular lamellae are observed. The stripe-like or ring skeleton of B domains locates at the interface between A domains and C domains resulting in a nearly complete separation between them.

Figure 9 depicts $\langle R\rangle$, $\langle R_g^2\rangle$, $\langle a\rangle$ and $\langle b\rangle$ of symmetric $A_7B_7C_7$ copolymer film with varying $\varepsilon_{(AC)}/\varepsilon_{(AB)}$, here $\langle a\rangle$ and $\langle b\rangle$ are the average length and width when the copolymer chain is viewed in terms of a spheroid. As shown in figure 9, there is a notable growth of $\langle R\rangle$ and $\langle R_g^2\rangle$ along with the increase of $\varepsilon_{(AC)}/\varepsilon_{(AB)}$, which indicates the enhanced stretching of copolymer chains. The trend of the length $\langle a\rangle$ is similar to that of $\langle R\rangle$ and $\langle R_g^2\rangle$. On the other hand, the width $\langle b\rangle$ of the spheroid decreases as the increase of $\varepsilon_{(AC)}/\varepsilon_{(AB)}$. The breadth $\langle c\rangle$ of the shortest semi-axes is too small to be calculated accurately, which hints that the spheroid of copolymer chain is nearly ellipse-like. In additional, the ellipse could be judged to parallel the fat surface. The parameters a, b and c contains more information about the chain conformations than that of $\langle R\rangle$ and $\langle R_g^2\rangle$, it is seen from figure 9 that the asphericity and crispation increases with increasing $\varepsilon_{(AC)}/\varepsilon_{(AB)}$ as a increases while b decreases.

It is known that the "bridge" configuration of ABC chains has strong influence on the mechanical properties. Here a conformational parameter, f_{bridge}, percentage of the "bridge" configuration proposed by Huh and Jo [33] is adopted to characterize the shape of the chains.

It is shown in figure 10 that when $\varepsilon_{(AC)}/\varepsilon_{(AB)} = -0.3333$, the two kinds of end blocks attracts each other, f_{bridge} is merely 0.45, more than one half of ABC copolymer chains take the "loop" configuration. It is why that the values of $\langle R\rangle$, $\langle R_g^2\rangle$ and $\langle a\rangle$ are comparatively small at negative $\varepsilon_{(AC)}/\varepsilon_{(AB)}$.

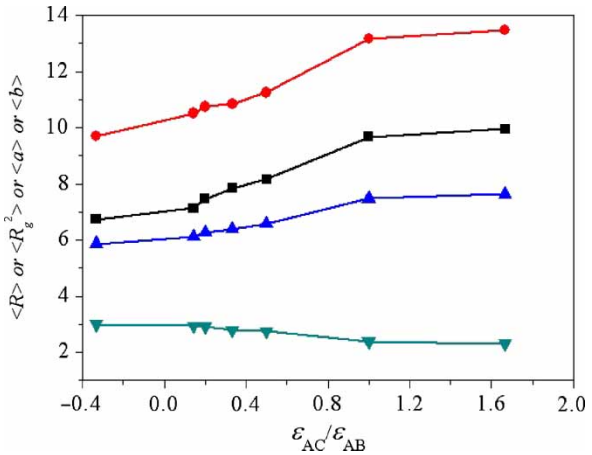

Figure 9. The relations of $\langle R\rangle$, $\langle R_g^2\rangle$, $\langle a\rangle$ and $\langle b\rangle$ with varying $\varepsilon_{(AC)}/\varepsilon_{(AB)}$. ■: $\langle R\rangle$; ●: $\langle R_g^2\rangle$; ▲: $\langle a\rangle$; ▼: $\langle b\rangle$.

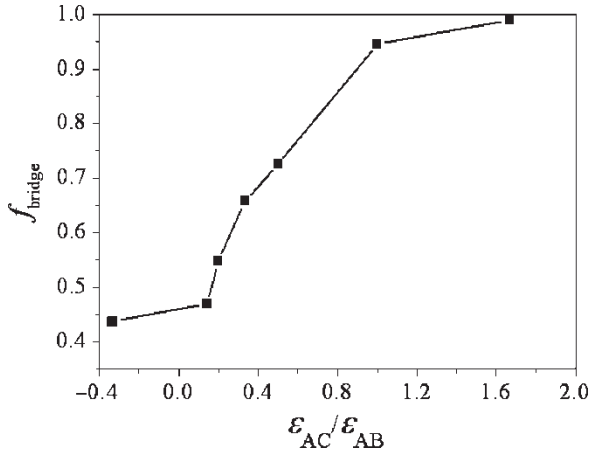

Figure 10. The percentage of "bridge" configuration of $A_7B_7C_7$, f_{bridge} vs. $\varepsilon_{(AC)}/\varepsilon_{(AB)}$.

However, when the interaction between end blocks A and C is repulsive, f_{bridge} increases with the increase of $\varepsilon_{(AC)}/\varepsilon_{(AB)}$ sharply. In the [0.0,1.0] interval of $\varepsilon_{(AC)}/\varepsilon_{(AB)}$, f_{bridge} jumps up from 0.5 to 0.95. After $\varepsilon_{(AC)}/\varepsilon_{(AB)} > 1.0$, the rising of f_{bridge} becomes mild where nearly all the copolymer chains take the "bridge" configurations. The statistical results in f_{bridge} vs. $\varepsilon_{(AC)}/\varepsilon_{(AB)}$ show good consistency with the curves of $\langle R\rangle$, $\langle R_g^2\rangle$ and $\langle a\rangle$ in figure 9. Also we can explain that the decline of $\langle b\rangle$ profile with the increase of $\varepsilon_{(AC)}/\varepsilon_{(AB)}$ is main responsible to the dominating "bridge" configuration, which results in the longer and the more compressive ellipse. Lee and Kim [36] studied the change of the long period (D) and the order–disorder transition temperature (T_{ODT}) of polystyrene-block-poly-(2-vinylpyridine) (PS-P2VP) and polystyrene-block-poly-(4-vinylpyridine) (PS-P4VP) with amount of cadmium chloride ($CdCl_2$) by rheology, synchrotron small-angle X-ray scattering (SAXS), and transmission electron microscopy (TEM). In their work, a small additive of metal halide was introduced to nitrogen atom in poly-(vinylpyridine) (PVP) with the aim to change the compatibility between the blocks. The type of coordination between metal halide and nitrogen atom changes with the position of nitrogen in PVP chains, which would give rise to a significant change in chain conformation further: intermolecular coordination for P4VP chains but intramolecular coordination for P2VP chains. Even though the diblock copolymer PS-PVP, which behaves differently from the triblock copolymer, is referred to in their paper, simulated results in this work are still proved to be consistent to their experiments on the examination from the chain conformation and interaction potential between the blocks

Figure 11 depicts the distribution of the probability of the angle ϕ, where ϕ is the angle between the vector from the mass center of block B to that of block A and the vector from the mass center of block B to that of block C, and $\langle P(\phi)\rangle$ as a function of the statistical probability of chains configuration at ϕ is employed. Glancing over figure 11 roughly, we can see that the $\langle P(\phi)\rangle$ profile of low $\varepsilon_{(AC)}/\varepsilon_{(AB)}$ fluctuates weaker than that of large $\varepsilon_{(AC)}/\varepsilon_{(AB)}$. The low angle interval of [0°,90°] corresponds to "loop"

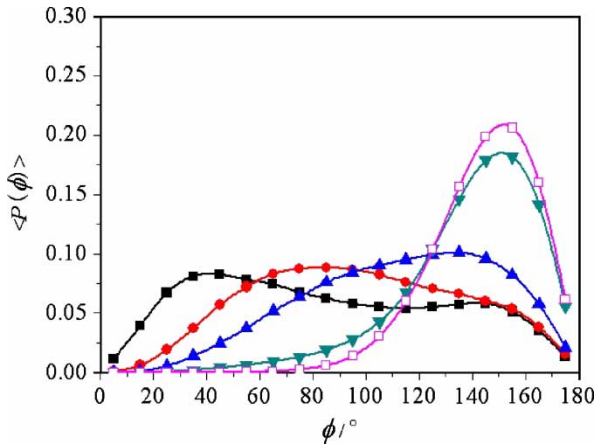

Figure 11. The distribution of $\langle P(\phi)\rangle$ as varied $\varepsilon_{(AC)}/\varepsilon_{(AB)}$. ■: $\varepsilon_{(AC)}/\varepsilon_{(AB)} = -0.3333$; ●: $\varepsilon_{(AC)}/\varepsilon_{(AB)} = 0.2$; ▲: $\varepsilon_{(AC)}/\varepsilon_{(AB)} = 0.5$; ▼: $\varepsilon_{(AC)}/\varepsilon_{(AB)} = 1.0$; □: $\varepsilon_{(AC)}/\varepsilon_{(AB)} = 1.6667$.

configuration, while $\phi > 90°$ indicates the "bridge" configuration. It is shown from the figure that the position of the peak of the $\langle P(\phi)\rangle$ moves towards the high angle interval with the increase $\varepsilon_{(AC)}/\varepsilon_{(AB)}$. Keeping on enhancing the repulsive interaction $\varepsilon_{(AC)}$, the peak of $\langle P(\phi)\rangle$ is shifted to high ϕ, and the probability of $\phi \leq 90°$ declined notably. This hints that the "bridge" configuration is gradually enhanced and finally dominating the micro-phase morphologies of the copolymer film when $\varepsilon_{(AC)}/\varepsilon_{(AB)} > 1.0$.

Figure 12(a) is a qualitative sketch map of the configuration of chains when $\varepsilon_{(AC)}/\varepsilon_{(AB)}$ is negative, corresponding to the morphology in figure 8(a). Figure 12(b) is that when $\varepsilon_{(AC)}$ is slight repulsive, corresponding to the morphology in figure 8(b) where the disordered "tricolor checkerboard-like" morphology is observed due to the increase of "bridge" configuration chains. Rich phase regions of different kinds of blocks form individually, the angle ϕ of copolymer chains distributed evenly in the interval of [60°,100°]. For a larger repulsive $\varepsilon_{(AC)}$ as shown in figure 12(c), corresponding to figure 8(c), the angle ϕ is higher than 120°, the most of copolymer chains stretch and parallel to the (x, y) planes, which causes the formation of perpendicular lamellae structure.

5. Conclusion

In this work, the micro-phase morphologies of ABC triblock copolymer ultra-thin film confined between two neutral hard walls were studied via Monte Carlo (MC) simulation on simple cubic lattice. When the film is ultra-thin due to the small L_z/N, the micro-phase structures of ABC triblock copolymer are dependent on not only the volume fraction f_B, but also the interaction ratio $\varepsilon_{(AC)}/\varepsilon_{(AB)}$. The sketch maps of the molecular orientations or the chain configurations were used to elucidate the formation of micro-phase separation of ABC triblock copolymer film intuitively on the respective condition of the various f_B and the different $\varepsilon_{(AC)}/\varepsilon_{(AB)}$.

When f_B is small, the copolymer chains are stretched parallel and distributed uniformly through the whole ultra-thin film. It is why the perpendicular lamellar structures form. In contrast, when f_B is large, lots of mass centers of chains are located at the middle layers of the film and stretched relative perpendicularly. Additionally, only a little of copolymer chains nearby the two walls align parallel to the (x, y) planes. The relative perpendicular copolymer chains shrink to some extent because of the repulsion from the hard walls. Combining the two kinds of orientations, the perforated lamellae of rich-B phase in the middle layers is formed finally.

When the interaction between end blocks A and C is attractive, A and C will embed each other and form a strip structure, no micro-phase separation between A segments

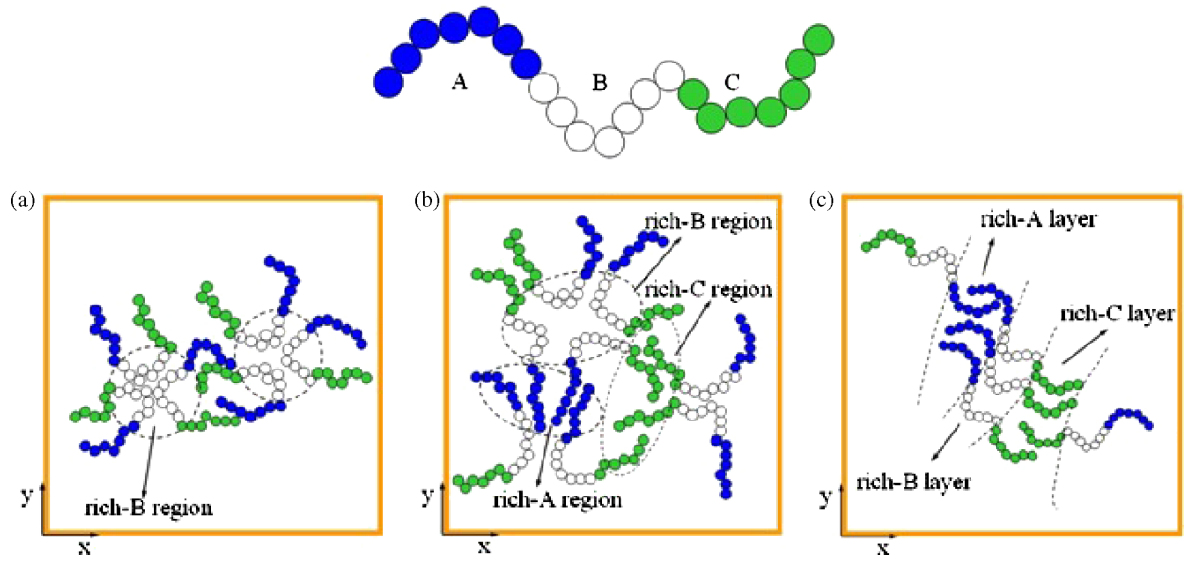

Figure 12. The sketch maps of the chain configurations and micro-phase morphologies.

and C segments occurs. The middle block B is completely isolated into several rich phase regions. Most of the ABC copolymer chains take on a "loop" configuration and shrink at low angle ϕ. While at the slight repulsive $\varepsilon_{(AC)}$, the disordered morphology of "tricolor checkerboard-like" would form due to the increase of the "bridge" configuration chains. Rich phase regions of different kinds of blocks form dispersedly, and the angle ϕ of copolymer chains distributes uniformly in the interval of [60°,100°]. For a larger repulsive $\varepsilon_{(AC)}$, the angle ϕ of copolymer chains is higher than 120°, and most of the copolymer chains stretch and parallel to the (x, y) planes, which causes the formation of a perpendicular lamellae structure.

Acknowledgements

This work is supported by the National Natural Science Foundation of China (Projects No. 20606010, 20490204), E-Institute of Shanghai High Institution Grid (No.200303) and Shanghai Municipal Science and Technology Commission of China (No.05DJ14002).

References

[1] I. Goodman. *Development in Block Copolymers*, Applied Sciences, New York (1982).
[2] M.J. Folks. *Processing, Structure and Properties of Block Copolymers*, Elsevier, New York (1985).
[3] P.R.L. Malenfant, L. Groenendaal, J.M.J. Frechet. Well-defined triblock hybrid dendrimers based on lengthy oligothiophene cores and poly(benzyl ether) dendrons. *J. Am. Chem. Soc.*, **120**, 10990 (1998).
[4] N. Minoura, M. Higuchi. Microphase-separated structure in triblock copolypeptide membranes composed of L-glutamic acid and L-leucine. *Macromolecules*, **30**, 1023 (1997).
[5] A. Urbas, Y. Fink, E.L. Thomas. One-dimensionally periodic dielectric reflectors from self-assembled block copolymer-homopolymer blends. *Macromolecules*, **32**, 4748 (1999).
[6] A.H. Trinh, H.H. Le, A. Rameshwar, W. Roland, G.H. Michler, K. Knoll. Influence of interfacial structure on morphology and deformation behavior of SBS block copolymers. *Polymer*, **44**, 1237 (2003).
[7] R. Krishnamoorti, M.A. Modi, M.F. Tse, H.C. Wang. Pathway and kinetics of cylinder-to-sphere order–order transition in block copolymers. *Macromolecules*, **33**, 3810 (2000).
[8] T. Miyamoto, K. Kodama, K. Shibayama. Structure and properties of a styrene–butadiene–styrene block copolymer. *J. Polym. Sci. A*, **8**, 2059 (1970).
[9] R.D. Peters, X.M. Yang, P.F. Nealey. Morphology of thin films of diblock copolymers on surfaces micropatterned with regions of different interfacial energy. *Macromolecules*, **35**, 1822 (2002).
[10] A. Budkowski, A. Bernasik, P. Cyganik, J. Raczkowska, B. Penc, B. Bergues, K. Kowalski, J. Rysz, J. Janik. Substrate-determined shape of free surface profiles in spin–cast polymer blend films. *Macromolecules*, **36**, 4060 (2003).
[11] A. Avgeropoulos, B.J. Dair, N. Hadjichristidis, E.L. Thomas. Tricontinuous double gyroid cubic phase in triblock copolymers of the ABA type. *Macromolecules*, **30**, 5634 (1997).
[12] T. Xu, Y. Zhu, S.P. Gido, T.P. Russell. Electric field alignment of symmetric diblock copolymer thin films. *Macromolecules*, **37**, 2625 (2004).
[13] H. Nakazawa, T. Ohta. Microphase separation of ABC-type triblock copolymers. *Macromolecules*, **26**, 5503 (1993).
[14] M.W. Matsen. Gyroid versus double-diamond in ABC triblock copolymer melts. *J. Chem. Phys.*, **108**, 785 (1998).
[15] X.F. Ren, J.C. Wei. Triblock copolymer theory: free energy, disordered phase and weak segregation. *Physica D.*, **178**, 103 (2003).
[16] J. Feng, E. Ruckenstein. Monte Carlo simulation of triblock copolymer thin films. *Polymer*, **43**, 5775 (2002).
[17] Y.M. Huang, H.L. Liu, Y. Hu. Monte Carlo simulations of the morphologies and conformations of triblock copolymer thin films. *Macromol. Theory Simul.*, **15**, 117 (2006).
[18] M.W. Matsen. Thin films of block copolymer. *J. Chem. Phys.*, **106**, 7781 (1997).
[19] M.W. Matsen, R.B. Thompson. Equilibrium behavior of symmetric ABA triblock copolymer melts. *J. Chem. Phys.*, **111**, 7139 (1999).
[20] Q. Wang, Q.L. Yan, P.F. Neeley, J.J. de Pablo. Monte Carlo simulations of diblock copolymer thin films confined between two homogeneous surfaces. *J. Chem. Phys.*, **112**, 450 (2000).
[21] Y. Xuan, J. Peng, L. Cui, H. Wang, B. Li, Y. Han. Morphology development of ultrathin symmetric diblock copolymer film via solvent vapor treatment. *Macromolecules*, **37**, 7301 (2004).
[22] I. Carmesin, K. Kremer. The bond fluctuation method: a new effective algorithm for the dynamics of polymers in all spatial dimensions. *Macromolecules*, **21**, 2819 (1988).
[23] R.G. Larson, L.E. Scriven, H.T. Davis. Monte Carlo simulation of model amphiphile-oil-water systems. *J. Chem. Phys.*, **83**, 2411 (1985).
[24] R.G. Larson. Self-assembly of surfactant liquid crystalline phases by Monte Carlo simulation. *J. Chem. Phys.*, **91**, 2479 (1989).
[25] J. Reiter, T. Edling, T. Pakula. Monte Carlo simulation of lattice models for macromolecules at high densities. *J. Chem. Phys.*, **93**, 837 (1990).
[26] C. Mischler, J. Baschnagel, K. Binder. Polymer films in the normal-liquid and supercooled state: a review of recent Monte Carlo simulation results. *Adv. Colloid Interface Sci.*, **94**, 197 (2001).
[27] A. Yethiraj, C.K. Hall. Monte Carlo simulation of polymers confined between flat plates. *Macromolecules*, **23**, 1865 (1990).
[28] A. Yethiraj. Monte Carlo simulation of confined semiflexible polymer melts. *J. Chem. Phys.*, **101**, 2489 (1994).
[29] M.R. Wilson, M.P. Allen. Computer simulation study of liquid crystal formation in a semi-flexible system of linked hard spheres. *Mol. Phys.*, **80**, 277 (1993).
[30] B. Fraser, C. Denniston, M.H. Müser. On the orientation of lamellar block copolymer phases under shear. *J. Chem. Phys.*, **124**, 104902 (2006).
[31] J. Yang, M.A. Winnik, T. Pakula. Interface orientation and chain conformation in simulated symmetric diblock copolymer lamellar systems. *Macromol. Theory Simul.*, **14**, 9 (2005).
[32] A. Böker, A. Knoll, H. Elbs, V. Abetz, A.H.E. Muller, G. Krausch. Large scale domain alignment of a block copolymer from solution using electric fields. *Macromolecules*, **35**, 1319 (2002).
[33] J. Huh, W.H. Jo, G. ten Brinke. Conformational analysis in ABA triblock melts by Monte Carlo simulation. *Macromolecules*, **35**, 2413 (2002).
[34] Q. Wang, Q.L. Yan, P.F. Nealey, J.J. de Pablo. Monte Carlo simulations of diblock copolymer thin films confined between two homogeneous surfaces. *J. Chem. Phys.*, **112**, 450 (2000).
[35] F.S. Bates, G.H. Fredrickson. Block copolymers-designer soft materials. Advances in synthetic chemistry and statistical theory provide unparalleled control over molecular scale morphology in this class of macromolecules. *Phys. Today*, **52**, 32 (1999).
[36] D.H. Lee, H.Y. Kim, J.K. Kim. Swelling and shrinkage of lamellar domain of conformationally restricted block copolymers by metal chloride. *Macromolecules*, **39**, 2027 (2006).